



HAL
open science

High-gain nonlinear observer with lower tuning parameter

Ali Zemouche, Fan Zhang, Frédéric Mazenc, Rajesh Rajamani

► **To cite this version:**

Ali Zemouche, Fan Zhang, Frédéric Mazenc, Rajesh Rajamani. High-gain nonlinear observer with lower tuning parameter. *IEEE Transactions on Automatic Control*, 2019, 64 (8), pp.3194-3209. 10.1109/TAC.2018.2882417 . hal-01936944

HAL Id: hal-01936944

<https://hal.science/hal-01936944>

Submitted on 16 Dec 2021

HAL is a multi-disciplinary open access archive for the deposit and dissemination of scientific research documents, whether they are published or not. The documents may come from teaching and research institutions in France or abroad, or from public or private research centers.

L'archive ouverte pluridisciplinaire **HAL**, est destinée au dépôt et à la diffusion de documents scientifiques de niveau recherche, publiés ou non, émanant des établissements d'enseignement et de recherche français ou étrangers, des laboratoires publics ou privés.

High-Gain Nonlinear Observer with Lower Tuning Parameter

A. ZEMOUCHE^{1,2}, F. ZHANG³, F. MAZENC², R. RAJAMANI⁴

Abstract—This paper develops a new high-gain observer design method for nonlinear systems that has a lower gain compared to the standard high-gain observer. This new observer, called HG/LMI observer is obtained by combining the standard high-gain methodology with the LMI-based observer design technique. Through analytical developments, the paper shows how the new observer provides lower gains, shows how it applies to systems with multi nonlinear functions and analyzes performance in the presence of measurement noise and/or delayed output measurements. A numerical example is given to illustrate the increasing advantage of the new HG/LMI observer with increase in the observer’s ‘compromise index’. Finally, the applicability and performance of the observer is demonstrated for a real-world application consisting of a train’s magnetic levitation system.

Index Terms—Observer design, high-gain methodology, Lipschitz systems, LMIs.

I. INTRODUCTION

NONLINEAR state observers have attracted much attention from the automatic control community in recent years [1], [2], [3], [4], [5], [6], [7]. Observers are needed since the full state cannot be measured or is too expensive to measure in many applications. For instance, slip angle and roll angle are too expensive to measure and have to be estimated from other inexpensive sensors in intelligent vehicle applications [8], [9]. The design of fault diagnostic systems also often requires the use of one or more exponentially stable observers [10]. In addition, some variables in many applications have to be estimated and cannot be measured due to unavailability of sensors at any cost.

Because of the lack of a single powerful observer design method for nonlinear systems (unlike the linear case), several different methods have been developed in the literature, where each method corresponds to design for a specific class of nonlinear systems. We can quote the class of systems with Lipschitz nonlinearities [11], [12], [13], [14], [15], [16]. Specifically for this class of systems many LMI techniques have been developed in the literature. Each new LMI technique aims to provide a better way to get less conservative LMI conditions compared to previous results. Despite theoretical advances in this field and although some enhancements have

been proposed recently [17], [18], [19], the problem still remains open.

Different from the LMI methods, another popular method for state estimation of nonlinear systems is the well known high-gain observer. The high-gain observer is developed for systems in triangular form or any system that can be transformed into a triangular structure. The advantage of the high-gain methodology is that it always guarantees the existence of an exponentially convergent observer, thanks to the tuning of only one parameter that should be chosen large enough [3], [20]. Although the practicability of high-gain observer in output feedback control has been nicely demonstrated by Khalil’s work [5], [21], the use of a large gain remains a major drawback. Indeed, a high-gain observer is very sensitive to output measurement noise because of the value of the tuning parameter which may be huge for higher dimensional systems having nonlinearities with large Lipschitz constants. To overcome this obstacle, many research papers have addressed high-gain observers with time-varying parameter adaptation, and a lot of schemes have been proposed. For an overview of the literature, we refer the reader to [22], [23], [17], [24], [25], [26], [27], and the references therein.

Despite all these improvements, the research activities in this direction still remain active and many problems remain to be solved to improve the performance of the high-gain observer with respect to measurement noise. A new technique was proposed in [28] to solve this problem. Through elegant arguments, the authors have proposed a high-gain observer with limited gain power. Their observer structure is new and different from the standard high-gain structure. Indeed, for an n -dimensional system, instead of a Luenberger observer structure of dimension n , they designed an observer of dimension $2n - 2$. Even if their gain power is limited to 2 instead of n with the standard high-gain, the higher dimension of the observer ($2n - 2$) may increase the size of the tuning parameter. As shown in [28], overall, this new high-gain observer is better than the standard one from the sensitivity to measurement noise point of view.

What we propose in this paper is different from the approach in [28]. Our technique follows the standard high-gain methodology with the same state observer structure of dimension n . However, by exploiting the LPV/LMI technique developed in [18], we are able to decrease the tuning parameter (then implicitly, the gain power is decreased). We will introduce a so called “*compromise index*” j_0 , with $0 \leq j_0 \leq n$. Hence, the power of the proposed high-gain is limited to j_0 , but we need to solve 2^{j_0} LMIs instead of one with the standard high-gain observer. The designed observer is called “*HG/LMI observer*”. In addition to the power gain limitation,

¹ University of Lorraine, CRAN CNRS UMR 7039, 54400 Cosnes et Romain, France (email: ali.zemouche@univ-lorraine.fr).

² EPI Inria DISCO, Laboratoire des Signaux et Systèmes, CNRS-CentraleSupélec, 91192 Gif-sur-Yvette, France (email: frederic.mazenc@l2s.centralesupelec.fr).

³ School of Mathematics, Southeast University, Nanjing 210096, China (email: fan.zhang@seu.edu.cn, dr.fanzhang@outlook.com).

⁴ Laboratory for Innovations in Sensing, Estimation, and Control, Department of Mechanical Engineering, University of Minnesota, Minneapolis, USA. (email: rajamani@umn.edu).

the HG/LMI observer provides lower gain thanks to a particular decomposition of the nonlinearity of the system, which allows reducing the Lipschitz constant in some cases, which is directly and proportionally related to the high-gain tuning parameter. After analytical developments, a numerical example with a comparison to the standard high gain observer and the Astolfi/Marconi observer is first presented to demonstrate the role of the index j_0 and its influence on decreasing the high-gain. Then, the applicability and performance of the observer in a real world application consisting of a magnetic levitation system is explored. Comparisons to the above mentioned high-gain observers is provided, where we clearly show the superiority of the proposed HG/LMI technique.

It is worth noticing that a short version of this work has been presented in the conference paper [29], where only a preliminary idea of the proposed technique was provided. However, this present journal version contains the additional material summarized in the following items:

- Advantages of the proposed HG/LMI observer are clearly described in Section IV-A;
- A numerical implementation algorithm is added in Section IV-B to show how the observer parameters are to be computed;
- Extension to systems with multi-nonlinearities is given in Section IV-C to widen the class of systems to which the observer design methodology is applicable;
- Robustness and performance analysis to delayed outputs and high-frequency measurement noise is included in Section V;
- An application to a magnetic levitation system of trains is included in Section VII to show the applicability of the proposed new design technique on real-world models;
- Comparisons to Astolfi/Marconi observer have been added in Sections VI and VII.

II. PROBLEM FORMULATION

A. Preliminaries

We start by introducing some definitions and preliminaries which will be of crucial use in the developed LPV-approach for Lipschitz and not necessarily differentiable systems.

Definition 1 ([18]). *Consider two vectors*

$$X = \begin{pmatrix} x_1 \\ \vdots \\ x_n \end{pmatrix} \in \mathbb{R}^n \text{ and } Z = \begin{pmatrix} z_1 \\ \vdots \\ z_n \end{pmatrix} \in \mathbb{R}^n.$$

For all $i = 0, \dots, n$, we define an auxiliary vector $X^{Z^i} \in \mathbb{R}^n$ corresponding to X and Z as follows:

$$\left\{ \begin{array}{l} X^{Z^i} = \begin{pmatrix} z_1 \\ \vdots \\ z_i \\ x_{i+1} \\ \vdots \\ x_n \end{pmatrix} \text{ for } i = 1, \dots, n \\ X^{Z^0} = X \end{array} \right. \quad (1)$$

Lemma 1 ([18]). *Consider a continuous function $\Psi : \mathbb{R}^n \rightarrow \mathbb{R}$. Then, for all*

$$X = \begin{pmatrix} x_1 \\ \vdots \\ x_n \end{pmatrix} \in \mathbb{R}^n \text{ and } Z = \begin{pmatrix} z_1 \\ \vdots \\ z_n \end{pmatrix} \in \mathbb{R}^n,$$

there exist functions $\psi_j : \mathbb{R}^n \times \mathbb{R}^n \rightarrow \mathbb{R}$, $j = 1, \dots, n$ so that

$$\Psi(X) - \Psi(Z) = \sum_{j=1}^{j=n} \psi_j \left(X^{Z^{j-1}}, X^{Z^j} \right) e_n^\top(j) (X - Z), \quad (2)$$

where $e_n(j)$ is the j^{th} vector of the canonical basis of \mathbb{R}^n .

Lemma 2 ([18]). *Consider a function $\Psi : \mathbb{R}^n \rightarrow \mathbb{R}^n$. Then, the two following items are equivalent:*

- Ψ is γ_Ψ -Lipschitz with respect to its argument, i.e.:

$$\left\| \Psi(X) - \Psi(Z) \right\| \leq \gamma_\Psi \left\| X - Z \right\|, \quad \forall X, Z \in \mathbb{R}^n; \quad (3)$$

- for all $i, j = 1, \dots, n$, there exist functions

$$\psi_{ij} : \mathbb{R}^n \times \mathbb{R}^n \rightarrow \mathbb{R}$$

and constants $\underline{\gamma}_{\psi_{ij}} \leq 0$, $\bar{\gamma}_{\psi_{ij}} \geq 0$, so that $\forall X, Z \in \mathbb{R}^n$,

$$\Psi(X) - \Psi(Z) = \sum_{i=1}^{i=n} \sum_{j=1}^{j=n} \psi_{ij} H_{ij} (X - Z), \quad (4)$$

and

$$-\gamma_\Psi \leq \underline{\gamma}_{\psi_{ij}} \leq \psi_{ij} \leq \bar{\gamma}_{\psi_{ij}} \leq \gamma_\Psi, \quad (5)$$

where

$$\psi_{ij} \triangleq \psi_{ij} \left(X^{Z^{j-1}}, X^{Z^j} \right) \text{ and } H_{ij} = e_n(i) e_n^\top(j).$$

B. System Description

Since this paper deals with high-gain observers, we will consider a special class of nonlinear systems. For simplicity of the presentation and to explain well what we propose in this paper, we consider the class of systems which are diffeomorphic to the form of the system studied in [3]:

$$\left\{ \begin{array}{l} \dot{x} = \begin{bmatrix} \dot{x}_1 \\ \dot{x}_2 \\ \vdots \\ \dot{x}_{n-1} \\ \dot{x}_n \end{bmatrix} = \begin{bmatrix} x_2 \\ x_3 \\ \vdots \\ x_n \\ f(x) \end{bmatrix} \\ y = x_1 \end{array} \right. \quad (6)$$

with $f : \mathbb{R}^n \rightarrow \mathbb{R}$ satisfying the Lipschitz property formulated under the following form:

$$\left| f(x_1 + \Delta_1, \dots, x_n + \Delta_n) - f(x_1, \dots, x_n) \right| \leq \gamma_f \sum_{j=1}^n |\Delta_j|. \quad (7)$$

For the sake of compactness, we write system (6) under the form:

$$\left\{ \begin{array}{l} \dot{x} = Ax + Bf(x) \\ y = Cx \end{array} \right., \quad (8)$$

where

$$B = [0 \ \dots \ 0 \ 1]^T, \quad C = [1 \ 0 \ \dots \ 0] \quad (9)$$

and the state matrix A is defined by

$$(A)_{i,j} = \begin{cases} 1 & \text{if } j = i + 1 \\ 0 & \text{if } j \neq i + 1 \end{cases}. \quad (10)$$

Consider the following Luenberger observer:

$$\dot{\hat{x}} = A\hat{x} + Bf(\hat{x}) + L(y - C\hat{x}). \quad (11)$$

The dynamics of the estimation error $\tilde{x} = x - \hat{x}$ is then given by:

$$\dot{\tilde{x}} = (A - LC)\tilde{x} + B[f(x) - f(\hat{x})]. \quad (12)$$

C. LPV/LMI-Based Approach

Since $f(\cdot)$ is γ_f -Lipschitz, then following Lemma 2 there are functions

$$\underline{\gamma}_j : \mathbb{R}^n \times \mathbb{R}^n \longrightarrow \mathbb{R}$$

and constants $\underline{\gamma}_{\gamma_j}$ and $\bar{\gamma}_{\gamma_j}$, so that

$$f(x) - f(\hat{x}) = \left[\sum_{j=1}^{j=n} \psi_j e_n^\top(j) \right] e, \quad (13)$$

and

$$\underline{\gamma}_{\gamma_j} \leq \psi_j \leq \bar{\gamma}_{\gamma_j}, \quad (14)$$

where

$$\psi_j \triangleq \psi_j(x_k^{\hat{x}_{j-1}}, x_k^{\hat{x}_j})$$

is defined as in Lemma 2. For the sake of brevity, we use only ψ_j instead of $\psi_j(x_k^{\hat{x}_{j-1}}, x_k^{\hat{x}_j})$.

Now, define the matrix function

$$\mathcal{A}(\Psi) = A + B \sum_{j=1}^{j=n} \psi_j e_n^\top(j), \quad \forall \Psi \in \mathbb{R}^n. \quad (15)$$

Then, the dynamics (12) can be rewritten as

$$\dot{\tilde{x}} = [\mathcal{A}(\Psi) - LC] \tilde{x}. \quad (16)$$

According to (14), the vector parameter Ψ belongs to a bounded convex set \mathcal{H}_n for which the set of vertices is defined by:

$$\mathcal{V}_{\mathcal{H}_n} = \left\{ \Phi \in \mathbb{R}^n : \Phi_j \in \left\{ \underline{\gamma}_{\gamma_j}, \bar{\gamma}_{\gamma_j} \right\} \right\}. \quad (17)$$

At this stage, we can state the following theorem, which provides LMI conditions for observer design of Lipschitz systems.

Theorem II.1 ([18]). *The observer (11) is asymptotically convergent if there exist a symmetric positive definite matrix \mathcal{P} and a matrix \mathcal{R} of appropriate dimension so that the following LMI conditions hold:*

$$\begin{aligned} \mathcal{A}(\Phi)^T \mathcal{P} + \mathcal{P} \mathcal{A}(\Phi) - C^T \mathcal{R} - \mathcal{R}^T C < 0, \\ \forall \Phi \in \mathcal{V}_{\mathcal{H}_n}. \end{aligned} \quad (18)$$

Then, the observer gain is given by

$$L = \mathcal{P}^{-1} \mathcal{R}^T.$$

The proof can be achieved easily by using the quadratic Lyapunov function

$$V(\tilde{x}) = \tilde{x}^T \mathcal{P} \tilde{x}.$$

D. High-Gain Methodology

Here, we recall the basic high gain observer as in [20]. Basically, in the high-gain methodology, we write the observer gain L under the form:

$$L := T(\theta)K, \quad \theta \geq 1. \quad (19)$$

where

$$T(\theta) := \text{diag}(\theta, \dots, \theta^n) \text{ and } K \in \mathbb{R}^n.$$

In addition, the high-gain methodology focuses on the transformed estimation error

$$\hat{\tilde{x}} := T^{-1}(\theta)\tilde{x}, \quad (20)$$

where $T^{-1}(\theta)$ is the inverse of $T(\theta)$ given by

$$T^{-1}(\theta) = \text{diag}\left(\frac{1}{\theta}, \dots, \frac{1}{\theta^n}\right).$$

It is well-known that the dynamics of the error $\hat{\tilde{x}}$ is given by

$$\dot{\hat{\tilde{x}}} = \theta(A - KC)\hat{\tilde{x}} + \frac{1}{\theta^n} B \Delta f, \quad (21)$$

with

$$\Delta f := f(x) - f(x - T(\theta)\hat{\tilde{x}}).$$

From the Lipschitz condition (7) and the fact that $\theta \geq 1$, we can show as in [26] that there always exists a positive scalar constant k_f , independent of θ , so that

$$\|T^{-1}(\theta)B\Delta f\| \leq k_f \|\hat{\tilde{x}}\|. \quad (22)$$

Indeed, since

$$T^{-1}(\theta)B\Delta f = \frac{1}{\theta^n} B\Delta f \quad \text{and} \quad T(\theta)\hat{\tilde{x}} = \begin{pmatrix} \theta \hat{\tilde{x}}_1 \\ \vdots \\ \theta^j \hat{\tilde{x}}_j \\ \vdots \\ \theta^n \hat{\tilde{x}}_n \end{pmatrix}$$

then, we have

$$\|T^{-1}(\theta)B\Delta f\| = \frac{1}{\theta^n} |\Delta f| = \frac{1}{\theta^n} |f(\theta \hat{\tilde{x}}_1, \dots, \theta^n \hat{\tilde{x}}_n)|.$$

From (7), it follows that

$$\begin{aligned} \|T^{-1}(\theta)B\Delta f\| &= \frac{1}{\theta^n} |f(\theta \hat{\tilde{x}}_1, \dots, \theta^n \hat{\tilde{x}}_n)| \\ &\leq \frac{\gamma_f}{\theta^n} \sum_{j=1}^n \theta^j |\hat{\tilde{x}}_j| = \gamma_f \sum_{j=1}^n \frac{\theta^j}{\theta^n} |\hat{\tilde{x}}_j|. \end{aligned} \quad (23)$$

Since $\theta \geq 1$ and $1 \leq j \leq n$, then $\frac{\theta^j}{\theta^n} \leq 1$. Finally, from the inequality

$$\sum_{j=1}^n |\hat{\tilde{x}}_j| \leq n \sqrt{\sum_{j=1}^n |\hat{\tilde{x}}_j|^2} = n \|\hat{\tilde{x}}\|$$

we get (22) with $k_f = n\gamma_f$, which is independent from θ .

Consequently, by following the high-gain methodology we obtain the following theorem.

Theorem II.2 ([20]). *If there exist $P > 0$, $\lambda > 0$, Y , and $\theta \geq 1$ such that*

$$A^T P + P A - C^T Y - Y^T C + \lambda I < 0, \quad (24)$$

$$\theta > \theta_0 = \frac{2k_f \lambda_{\max}(P)}{\lambda}, \quad (25)$$

then the estimation error \tilde{x} is asymptotically stable for the choice

$$K = P^{-1} Y^T,$$

where $\lambda_{\max}(P)$ is the largest eigenvalue of the matrix P .

Proof. For more details about the proof of this theorem, we refer the reader to [20], [26], [27]. \square

E. Problem formulation and objectives

If the LPV/LMI based approach is the best LMI technique and avoids high-gain, it has a weakness from the complexity point of view. Indeed, to synthesize the observer gain, the LPV/LMI based approach typically needs to solve a high number of LMIs, $n_{\text{LMI}} = 2^n$. In addition, this technique, as is the case for all LMI techniques, contrary to the high-gain method, provides sufficient LMI conditions from which we cannot guarantee the existence of a stable observer before solving the LMIs. On the other hand, it is true that before solving conditions (24)-(25), the high-gain methodology guarantees convergence, however the obtained gain is really high even for Lipschitz constants not too large. This weakness affects strongly the performance of the high-gain observer, namely in the case of systems with noise measurement.

To overcome the above drawbacks, we propose to combine the two designs. We will exploit the advantages of each method to get a new and improved observer design technique. Especially, the combined observer, that we will call "HG/LMI observer" will have smaller observer gain compared to the standard high-gain. On the other hand, the number of LMIs n_{LMI} will be significantly decreased. Mainly we will reduce the value of the right hand side of the high-gain condition (25). To do this successfully, we will need to use the LPV/LMI based approach; then the new design method will reduce the number of LMIs related to the standard LPV/LMI technique. The next section is devoted to this issue.

III. PRELIMINARY RESULTS

A. Introduction and motivating example

The fact that k_f in inequality (22) is independent of θ is not necessarily an advantage. Indeed, this depends on how θ would be involved in k_f . Also, the fact that k_f is independent of θ does not come only from the condition $\theta \geq 1$, but essentially from the presence of the last component of x in f . Because of this last component, the parameter θ vanishes from the term $\frac{1}{\theta^n} \Delta f$ for $\theta \geq 1$. This can be shown easily by using the Lipschitz property (7). To illustrate this point and to motivate

our study, let us consider a simple three dimensional system. If we take a nonlinear function

$$f(x) = \gamma_f \sin(x_3),$$

then we get from (7)

$$\frac{1}{\theta^3} \|\Delta f\| \leq \frac{\gamma_f}{\theta^3} \times |\theta^3 \hat{x}_3| = \gamma_f |\hat{x}_3| \leq k_f \|\hat{x}\|,$$

where $k_f = \gamma_f$ in this case. However, if we take

$$f(x) = \gamma_f \sin(x_2),$$

then we get

$$\frac{1}{\theta^3} \|\Delta f\| \leq \frac{\gamma_f}{\theta^3} \times |\theta^2 \hat{x}_2| = \frac{\gamma_f}{\theta} |\hat{x}_2| \leq \frac{k_f}{\theta} \|\hat{x}\|.$$

Hence, by replacing in (25) k_f by $\frac{k_f}{\theta}$, θ_0 will be reduced to $\sqrt{\theta_0}$, which will reduce significantly the values of the observer gain.

The main result of this paper is based on the above idea. Thanks to the LPV/LMI technique combined with the standard high-gain methodology, we will be able to obtain a high-gain observer with a lower gain.

B. General case

This section is devoted to the preliminary key idea of the proposed work. The high gain methodology exploits the fact that k_f in (22) is independent of θ . Our key idea lies in this inequality. Indeed, under a simple assumption, we will show that we can obtain a lower high-gain. That is, the value of θ_0 in (25) will be reduced thanks to this assumption.

Assumption III.1. *There exists $j_0 > 0$ so that*

$$\frac{\partial f}{\partial x_j}(x) \equiv 0, \forall j > n - j_0. \quad (26)$$

This assumption means that the nonlinear function f does not depend on the j_0 last components of the state vector x . Notice that when Assumption III.1 is not fulfilled, we have $j_0 = 0$, which corresponds to the standard high-gain observer.

Under this assumption, inequality (22) becomes

$$\|T^{-1}(\theta) B \Delta f\| \leq \frac{k_{j_0}}{\theta^{j_0}} \|\hat{x}\|, \quad (27)$$

where k_{j_0} is independent of θ and $k_{j_0} \leq k_f$, where k_f is the same than that in (22). It is clear that with inequality (27), we reduce significantly the value of θ_0 . Therefore, we get the following theorem providing our preliminary result, which is the key idea of this paper.

Theorem III.2. *Under Assumption III.1, if there exist $P > 0$, $\lambda > 0$, Y , and $\theta \geq 1$ such that*

$$A^T P + P A - C^T Y - Y^T C + \lambda I < 0, \quad (28)$$

$$\theta^{1+j_0} > \theta_{j_0} = \frac{2k_{j_0} \lambda_{\max}(P)}{\lambda}, \quad (29)$$

then the estimation error \tilde{x} is asymptotically stable with

$$K = P^{-1} Y^T.$$

As can be shown in (29), the value θ_0 is decreased to $\theta_{j_0}^{\frac{1}{1+j_0}}$, which is a very significant attenuation of the standard high-gain.

C. HG/LMI Observer: preliminary result

This section is devoted to the preliminary contribution of this paper for systems with a single nonlinearity. We will exploit the LPV/LMI based technique to extend the previous result to systems which do not satisfy Assumption III.1.

Following (13), Δf in (21) can be rewritten under the following form:

$$\Delta f = \underbrace{\sum_{j=1}^{n-j_0} \psi_j \hat{x}_j}_{\Delta f_1} + \underbrace{\sum_{j=1}^{j_0} \psi_{k(j)} \hat{x}_{k(j)}}_{\text{for LPV/LMI}}, \quad (30)$$

where

$$k(j) = n - (j_0 - j),$$

$$0 \leq j_0 \leq n.$$

Hence, the error dynamics (21) is rewritten as follows:

$$\dot{\hat{x}} = \theta \left(\mathcal{A}(\Psi^\theta) - KC \right) \hat{x} + \frac{1}{\theta^n} B \Delta f_1, \quad (31)$$

where

$$\mathcal{A}(\Psi^\theta) = A + B \sum_{j=1}^{j_0} \psi_j^\theta e_n^\top(k(j)), \quad (32)$$

$$\Psi^\theta = \begin{pmatrix} \psi_1^\theta \\ \vdots \\ \psi_{j_0}^\theta \end{pmatrix} \in \mathbb{R}^{j_0}, \quad (33)$$

$$\psi_j^\theta = \frac{\psi_{k(j)}}{\theta^{1+(j_0-j)}}. \quad (34)$$

Now define the convex bounded set

$$\mathcal{H}_{j_0}^\sigma = \left\{ \Phi \in \mathbb{R}^{j_0} : \frac{\underline{\gamma}_{\gamma_{k(j)}}}{\sigma^{1+(j_0-j)}} \leq \Phi_j \leq \frac{\bar{\gamma}_{\gamma_{k(j)}}}{\sigma^{1+(j_0-j)}} \right\} \quad (35)$$

for which the set of vertices is defined by

$$\mathcal{V}_{\mathcal{H}_{j_0}^\sigma} = \left\{ \Phi \in \mathbb{R}^{j_0} : \Phi_j \in \left\{ \frac{\underline{\gamma}_{\gamma_{k(j)}}}{\sigma^{1+(j_0-j)}}, \frac{\bar{\gamma}_{\gamma_{k(j)}}}{\sigma^{1+(j_0-j)}} \right\} \right\}. \quad (36)$$

Since $\bar{\gamma}_{\gamma_{k(j)}} \geq 0$ and $\underline{\gamma}_{\gamma_{k(j)}} \leq 0$, then it is obvious that for two positive scalars σ_1, σ_2 , we have the following implication:

$$\sigma_1 < \sigma_2 \implies \mathcal{H}_{j_0}^{\sigma_1} \supset \mathcal{H}_{j_0}^{\sigma_2}. \quad (37)$$

Moreover,

$$\lim_{\sigma \rightarrow +\infty} \left(\mathcal{H}_{j_0}^\sigma \right) = \left\{ 0_{\mathbb{R}^{j_0}} \right\}. \quad (38)$$

On the other hand, we can show that there exists a positive real number $k_{j_0} \leq k_f$ so that Δf_1 satisfies

$$\|T^{-1}(\theta)B\Delta f_1\| \leq \frac{k_{j_0}}{\theta^{j_0}} \|\hat{x}\|. \quad (39)$$

Consequently, by analogy to Theorem III.2 and by using the convexity principle as in Theorem II.1, we obtain the following more general theorem.

Theorem III.3. *If there exist $P > 0$, $\lambda > 0$, Y , and $\sigma > 0$ such that*

$$\mathcal{A}(\Psi^\sigma)^T P + P \mathcal{A}(\Psi^\sigma) - C^T Y - Y^T C + \lambda I < 0, \forall \Psi^\sigma \in \mathcal{V}_{\mathcal{H}_{j_0}^\sigma}, \quad (40)$$

$$\theta^{1+j_0} > \theta_{j_0} = \frac{2k_{j_0} \lambda_{\max}(P)}{\lambda}, \quad (41)$$

then the estimation error \tilde{x} is asymptotically stable with

$$L = T(\theta) \overbrace{P^{-1} Y^T}^K, \quad \theta \geq \max \left(\sigma, \theta_{j_0}^{\frac{1}{1+j_0}} \right).$$

Proof. A direct application of Theorem III.2 leads to $\dot{V}(\hat{x}) < 0$, for all $\hat{x} \neq 0$, with $V(\hat{x}) = \hat{x}^\top P \hat{x}$, if

$$\mathcal{A}(\Psi^\theta)^T P + P \mathcal{A}(\Psi^\theta) - C^T Y - Y^T C + \lambda I < 0, \forall \Psi^\theta \in \mathcal{H}_{j_0}^\theta, \quad (42)$$

and

$$\theta^{1+j_0} > \theta_{j_0} = \frac{2k_{j_0} \lambda_{\max}(P)}{\lambda}. \quad (43)$$

At this stage, inequality (42) is not exploitable because it depends on θ . However, from the inclusion implication (37), we get $\Psi^\theta \in \mathcal{H}_{j_0}^\sigma$ for all $\theta \geq \sigma$. Hence from the convexity principle [30], inequality (42) holds if (40) is satisfied. Therefore, the observer gain

$$L = T(\theta) P^{-1} Y^T \quad (44)$$

ensures the exponential convergence of the estimation error towards zero for all θ such that

$$\theta \geq \max \left(\sigma, \theta_{j_0}^{\frac{1}{1+j_0}} \right). \quad (45)$$

This ends the proof. \square

IV. DISCUSSIONS AND EXTENSION

In this section, we will provide some discussions on the HG/LMI observer technique compared to the standard high-gain methodology and the LPV/LMI technique. A numerical design implementation will also be given. Then, an extension to systems with multi-nonlinearity will be provided in order to render the HG/LMI technique more interesting and applicable for a wider class of systems, like in the standard high-gain case.

A. On the advantages of HG/LMI observer

This section is devoted to some clarifications on the advantages of the proposed HG/LMI observer. We will clarify more the role of the so-called "compromise index" j_0 .

The advantages of the proposed HG/LMI technique can be summarized in the following items:

- The proposed technique can be viewed as a way to reduce the number of LMIs related to the LPV/LMI technique. Indeed, the number of LMI of LPV/LMI method is

reduced from 2^n to 2^{j_0} , which represents the number of vertices in the set $\mathcal{V}_{\mathcal{H}^{j_0}}$;

- The observer gain L of the HG/LMI technique is significantly smaller than that returned by the standard high-gain observer because of the power $\frac{1}{1+j_0}$ due to the compromise index j_0 ;
- The standard high-gain observer is a particular solution corresponding to $j_0 = 0$;
- The LPV/LMI observer is a particular solution corresponding to $j_0 = n$;
- Solutions with LPV/LMI method are always guaranteed. Indeed, there always exists $\sigma > 0$ so that the LMIs (40) admit solutions because from (38), we have

$$\lim_{\sigma \rightarrow +\infty} \left(\mathcal{A}(\Psi^\sigma) \right) = \mathcal{A} \left(\lim_{\sigma \rightarrow +\infty} (\Psi^\sigma) \right) = A. \quad (46)$$

This proves that the LPV/LMI technique for this class of systems with the high-gain structure can always provide solutions for the set of sufficient LMIs (40) for σ large enough. Indeed, from (46) and the continuity of $\mathcal{A}(\Psi^\sigma)$ with respect to σ , if (24) holds, we have

$$\begin{aligned} & \lim_{\sigma \rightarrow +\infty} \left(A(\Psi^\sigma)^T P + P A(\Psi^\sigma) - C^T Y - Y^T C + \lambda I \right) \\ &= \mathcal{A} \left(\lim_{\sigma \rightarrow +\infty} (\Psi^\sigma) \right)^T P + P \mathcal{A} \left(\lim_{\sigma \rightarrow +\infty} (\Psi^\sigma) \right) \\ & \quad - C^T Y - Y^T C + \lambda I \\ &= A^T P + P A - C^T Y - Y^T C + \lambda I < 0. \end{aligned} \quad (47)$$

Then, by definition of the limit, there exists σ_0 such that (40) is satisfied for any $\sigma > \sigma_0$. In addition, using the definition of $\mathcal{A}(\Psi^\sigma)$, we can show that the standard high-gain observer is a particular solution of (40). Indeed, from the construction of $\mathcal{A}(\Psi^\sigma)$, we can write

$$\mathcal{A}(\Psi^\sigma) = A + A_\sigma \quad \text{with} \quad \|A_\sigma\| \leq \frac{k_f}{\sigma}.$$

Then, the left term of inequality (40) satisfies the following inequality:

$$\begin{aligned} & \left(A^T P + P A - C^T Y - Y^T C + \lambda I \right) + A_\sigma^T P + P A_\sigma \\ & \leq \left(A^T P + P A - C^T Y - Y^T C + \lambda I \right) + \frac{2k_f \lambda_{\max}(P)}{\sigma} I. \end{aligned} \quad (48)$$

It follows that if (24) is satisfied (which is always feasible due to the observability canonical form), then there exists $\epsilon > 0$ so that

$$A^T P + P A - C^T Y - Y^T C + \lambda I \leq -\epsilon I.$$

Then, (48) holds for any $\sigma > \sigma_0 = \frac{2k_f \lambda_{\max}(P)}{\epsilon}$.

Table I sums up the number of LMIs, n_{LMI} , and the value of θ for each method: standard high-gain (Standard HG); LPV/LMI technique, and the combined HG/LMI method. Tables II, III and IV provide some examples for different values of n, θ_0 and j_0 .

Methods	Standard HG	LPV/LMI	HG/LMI
θ	θ_0	σ	$\theta \frac{1}{j_0^{1+j_0}}$
n_{LMI}	1	2^n	2^{j_0}

TABLE I
ILLUSTRATION OF THE HG/LMI METHOD

Methods	Standard HG	LPV/LMI	HG/LMI
θ	100	σ	10
n_{LMI}	1	$2^{10} = 1024$	2

TABLE II
 $n = 10, j_0 = 1$ AND $\theta_0 = 100$

Methods	Standard HG	LPV/LMI	HG/LMI
θ	1000	σ	10
n_{LMI}	1	$2^{10} = 1024$	4

TABLE III
 $n = 10, j_0 = 2$ AND $\theta_0 = 1000$

Methods	Standard HG	LPV/LMI	HG/LMI
θ	1000	σ	$\sqrt{10}$
n_{LMI}	1	$2^{10} = 1024$	8

TABLE IV
 $n = 10, j_0 = 3$ AND $\theta_0 = 1000$

B. Design algorithm: numerical implementation

In this section, we will present an algorithm which allows of synthesizing a gain K and a parameter σ . The algorithm we propose provides a simple and systematic numerical procedure for the design of a smaller gain L .

The parameter σ is generally not large, as can be shown through the comparisons in [12]. The simulations in [12] provide small gain K with $\sigma = 1$. We could take $\sigma = 1$ in (40). However, the parameter σ is introduced to guarantee the existence of solutions for (40). In addition, since the high-gain constraint (41) depends on P and (40) depends on σ and P , then even if the LMI (40) is feasible for $\sigma = 1$, it is always possible to find better and lower solutions for $\sigma > 1$. On the other hand, from homogeneity of (40)-(41), the decision variable λ can be fixed to $\lambda = 1$. As for the selection of σ , the best solution we found efficient for the numerical procedure is the use of the gridding method. For this, we introduce a bijective change of variable $\tau = \frac{\sigma}{1+\sigma}$ ($\sigma = \frac{\tau}{1-\tau}$). Hence when $\sigma \in [1, +\infty[$, the new variable $\tau \in [\frac{1}{2}, 1[$. Then we can use the gridding method on τ . The following algorithm summarizes the numerical design procedure we proposed to get a lower observer gain.

Algorithm 1: Design of an optimal gain L

- (i) Choose a small $\epsilon > 0$ for the gridding, take $\tau = \frac{1}{2}$, a high value $v_{\text{gain}} > 0$ and go to step (ii);

- (ii) Solve LMIs (40). If (40) is found feasible, then go to step (iv). Else go to step (iii);
- (iii) While $\tau + \epsilon < 1$, take $\tau := \tau + \epsilon$ and return to step (ii);
- (iv) Take $\theta = \max\left(\frac{\tau}{1-\tau}, \theta_{j_0}^{\frac{1}{1+\tau_0}}\right)$ and compute L as in (44). If $v_{gain} > \|L\|$, then put $v_{gain} := \|L\|$ and go to step (ii);

Algorithm 1 will be used in Section VI to show the performance of the new HG/LMI observer.

Remark 1. It should be noticed that, generally, there are two kinds of computational complexity: the first one is related to the on-line real-time computation and the second one is related to the numerical solving of the LMIs by using available LMI solvers. As for the first case, it should be noticed that the computation of the proposed HG/LMI observer parameters K , σ , and θ does not affect the on-line implementation of the algorithm because all these parameters are computed off-line; all the observer parameters are constant. As for the numerical solving of the proposed LMI conditions, the advantage of the proposed HG/LMI observer is the significant reduction of the number of LMIs to be solved, compared to the standard LPV/LMI method. As shown through the illustrative example in Section VI, solving only 2 LMIs, instead of 32 with the LPV/LMI-based technique, allows reducing significantly the values of the high-gain observer parameters. To sum up, there is no additional computation time for on-line real-time applications because all the observer parameters are constant and computed off-line. There is also no significant computation time related to the LMI solving, because the number of LMIs to be solved is significantly reduced compared to the LPV/LMI method.

C. Extension to systems with multi-nonlinearties

The HG/LMI method can be extended straightforwardly to systems described by the following equations:

$$\begin{cases} \dot{x} = \begin{bmatrix} x_2 + f_1(x_1) \\ x_3 + f_2(x_1, x_2) \\ \vdots \\ x_n + f_{n-1}(x_1, \dots, x_{n-1}) \\ f_n(x_1, \dots, x_n) \end{bmatrix} \\ y = x_1 = Cx \end{cases} \triangleq Ax + f(x), \quad (49)$$

where A and C are the matrices defined in (9)-(10), and the nonlinearities satisfy the following Lipschitz property:

$$|f_i(x_1 + \Delta_1, \dots, x_i + \Delta_i) - f_i(x_1, \dots, x_i)| \leq \sum_{j=1}^i k_j |\Delta_j|. \quad (50)$$

Remark 2. The systems studied in this paper are those which can be transformed into the observability canonical form (6) or (49) by mean of a diffeomorphism. Then, all the examples considered in this paper are observable: The

illustrative example considered in Section VI is observable; the magnetic levitation model in Section VII is uniformly observable because it is transformed into the observable canonical form (86) by mean of a diffeomorphism given in Appendix. Nevertheless, the results can be generalized to all uniformly observable systems:

$$\begin{cases} \dot{x} = \psi(x, u) \\ y = \phi(x, u) \end{cases}$$

that can be transformed, by mean of a diffeomorphic change of variables $z = \Phi(x)$, to the observability canonical form [31]:

$$\begin{cases} \dot{z}_i = f_i(z_1, \dots, z_{i+1}, u), & 1 \leq i \leq n-1 \\ \dot{z}_n = f_n(z, u) \\ y = h(z_1, u) \end{cases}$$

with

$$\frac{\partial h}{\partial z_1}(z_1, u) \neq 0,$$

$$\frac{\partial f_i}{\partial z_{i+1}}(z_1, \dots, z_{i+1}, u) \neq 0, \quad 1 \leq i \leq n-1.$$

The references [32] and [20] contain more explanations on how such a transformation exists.

Remark 3. The paper proposes to design a constant gain nonlinear observer based on the standard high-gain methodology [32] for systems represented in Euclidian space. All the mathematical developments and convergence aspects are performed in a Euclidian space. Although nonlinear systems are sometimes better represented in a Riemannian space, this issue is not raised in this paper. Constructing convenient Riemannian metrics may produce different results for observer design and lead to relevant conditions. For more details on the convergence of nonlinear observers with a Riemannian metric, we refer the reader to [33]. Some techniques to construct appropriate Riemannian metrics for nonlinear observer design can be found in [34], [35].

We consider the standard high-gain observer structure:

$$\dot{\hat{x}} = A\hat{x} + f(\hat{x}) + L(y - C\hat{x}), \quad (51)$$

where L is defined as in (19).

The dynamics of the transformed error $\hat{\hat{x}}$, defined in (20), is then given by:

$$\dot{\hat{\hat{x}}} = \theta(A - KC)\hat{\hat{x}} + T^{-1}(\theta)\Delta f \quad (52)$$

with

$$\Delta f := f(x) - f(x - T(\theta)\hat{\hat{x}}).$$

Each nonlinear component f_i can be written under an analogous form to (30):

$$\Delta f_i = \sum_{j=1}^{i-j_i} \theta^j \psi_{i_j} \hat{\hat{x}}_j + \sum_{j=1}^{j_i} \theta^{k_i(j)} \psi_{i_{k_i(j)}} \hat{\hat{x}}_{k_i(j)}, \quad (53)$$

where

$$\begin{aligned} k_i(j) &= i - (j_i - j), \\ 0 &\leq j_i \leq i. \end{aligned}$$

It follows that Δf is written as

$$\Delta f = \underbrace{\sum_{i=1}^n \sum_{j=1}^{i-j_i} \theta^j \psi_{ij} e_n(i) \hat{x}_j}_{\Delta f_1} \quad \text{for HG} \\ + \underbrace{\sum_{i=1}^n \sum_{j=1}^{j_i} \theta^{k_i(j)} \psi_{ik_i(j)} e_n(i) \hat{x}_{k_i(j)}}_{\text{for LPV/LMI}}. \quad (54)$$

$$\dot{\hat{x}} = \theta \left(\mathcal{A}(\Psi^\theta) - KC \right) \hat{x} + T^{-1}(\theta) \Delta f_1, \quad (55)$$

where

$$\mathcal{A}(\Psi^\theta) = A + B \sum_{i=1}^n \sum_{j=1}^{j_i} \psi_{ij}^\theta e_n(i) e_n^\top(k_i(j)), \quad (56)$$

$$\Psi^\theta = \begin{pmatrix} \psi_{11}^\theta \\ \vdots \\ \psi_{1j_1}^\theta \\ \psi_{21}^\theta \\ \vdots \\ \psi_{2j_2}^\theta \\ \vdots \\ \psi_{nj_n}^\theta \end{pmatrix} \in \mathbb{R}^{\sum_{i=1}^n j_i}, \quad (57)$$

$$\psi_{ij}^\theta = \frac{\psi_{ik_i(j)}}{\theta^{1+(j_i-j)}}. \quad (58)$$

As in the previous section (in the case with single nonlinear component), we define the bounded convex set

$$\mathcal{H}_{j_{\min}}^\sigma = \left\{ \Phi \in \mathbb{R}^{\sum_{i=1}^n j_i} : \frac{\underline{\gamma}_{\gamma_{ik_i(j)}}}{\sigma^{1+(j_i-j)}} \leq \Phi_{ij} \leq \frac{\bar{\gamma}_{\gamma_{ik_i(j)}}}{\sigma^{1+(j_i-j)}} \right\} \quad (59)$$

for which the set of vertices is defined by

$$\mathcal{V}_{\mathcal{H}_{j_{\min}}^\sigma} = \left\{ \Phi \in \mathbb{R}^{\sum_{i=1}^n j_i} : \Phi_{ij} \in \left\{ \frac{\underline{\gamma}_{\gamma_{ik_i(j)}}}{\sigma^{1+(j_i-j)}}, \frac{\bar{\gamma}_{\gamma_{ik_i(j)}}}{\sigma^{1+(j_i-j)}} \right\} \right\}, \quad (60)$$

where $\underline{\gamma}_{\gamma_{ik_i(j)}} \leq 0$ and $\bar{\gamma}_{\gamma_{ik_i(j)}} \geq 0$ are respectively, the lower and upper bounds of the bounded parameter $\psi_{ik_i(j)}$.

On the other hand, it is easy to show that there exists a constant $k_{j_{\min}}$ independent from θ such that the following holds:

$$\|T^{-1}(\theta) \Delta f_1\| \leq \frac{k_{j_{\min}}}{\theta^{\sum_{i=1}^n j_i}} \|\hat{x}\|. \quad (61)$$

Hence, by analogy, we get the next general theorem valid for systems with multi-nonlinearities.

Theorem IV.1. *If there exist $P > 0$, $\lambda > 0$, Y , and $\sigma > 0$ such that*

$$\mathcal{A}(\Psi^\sigma)^T P + P \mathcal{A}(\Psi^\sigma) - C^T Y \\ - Y^T C + \lambda I < 0, \forall \Psi^\sigma \in \mathcal{V}_{\mathcal{H}_{j_{\min}}^\sigma}, \quad (62)$$

$$\theta^{1+\min_{j_i \neq i} (j_i)} > \frac{2k_{j_{\min}} \lambda_{\max}(P)}{\lambda}, \quad (63)$$

then the estimation error \tilde{x} is asymptotically stable with

$$L = T(\theta) \overbrace{P^{-1} Y^T}^K, \quad (64)$$

$$\theta \geq \max \left(\sigma, \left[\frac{2k_{j_{\min}} \lambda_{\max}(P)}{\lambda} \right]^{\frac{1}{1+\min_{j_i \neq i} (j_i)}} \right). \quad (65)$$

Remark 4. *Notice that in such a case, the number of LMIs to be solved is*

$$n_{\text{LMI}} = \sum_{i=1}^n 2^{j_i}.$$

By following the reasoning in [36], this number of LMIs can be decreased to $n_{\text{LMI}} = 2 \sum_{i=1}^n j_i$.

Remark 5. *It is worth noticing that taking $j_i > \min_{j_i \neq i} (j_i)$ for some $i = 1, \dots, n$ does not affect $\theta_{j_i \neq i}^{\min(j_i)}$ in the inequality (61), but it may affect the value of $k_{j_{\min}}$. Hence, if the nonlinear component corresponding to $j_i > \min_{j_i \neq i} (j_i)$ does not increase significantly $k_{j_{\min}}$, then it is better to include it in Δf_1 instead of including it for the LPV/LMI part. Indeed, this leads to decrease n_{LMI} without affecting neither the LMIs (62) nor the high-gain constraint (63).*

V. ROBUSTNESS AND PERFORMANCE ISSUES

This section is devoted to some robustness issues. We will consider two cases: the first case deals with systems with delayed output measurements, while the second one raises the problem of high-frequency measurement noise.

A. Robustness to delay in the measurements

We consider the system

$$\begin{aligned} \dot{x}(t) &= Ax(t) + Bf(x(t)) \\ y(t) &= Cx(t - \tau) \end{aligned}, \quad (66)$$

where (A, C) and f satisfy the related assumptions of the previous sections. At least for the time being, we assume that $\tau > 0$ is known.

We consider the system

$$\dot{\hat{x}}(t) = A\hat{x}(t) + f(\hat{x}(t)) + L[y(t) - C\hat{x}(t - \tau)], \quad (67)$$

where L is defined as in (19).

Let us notice that the finite escape time phenomenon does not occur.

We have

$$\dot{\tilde{x}}(t) = A\tilde{x}(t) + f(x(t)) - f(\hat{x}(t)) - LC\tilde{x}(t - \tau). \quad (68)$$

Then, from (31), we can write

$$\dot{\tilde{x}}(t) = \left[\theta \left(\mathcal{A}^{j_0}(\Psi_{j_0}^\theta(t)) - KC \right) \hat{x} + \frac{1}{\theta^n} B \Delta f^{j_0} \right] \\ - LCT(\theta) \left(\hat{x}(t - \tau) - \hat{x}(t) \right). \quad (69)$$

Notice that $\dot{\hat{x}}$ can also be formulated as follows:

$$\dot{\hat{x}}(t) = \theta \mathcal{A}^n(\Psi_n^\theta(t)) \hat{x}(t) - LCT(\theta) \hat{x}(t - \tau). \quad (70)$$

These two formulations of the dynamics of the error \hat{x} are needed in what we propose in the next mathematical developments.

Now, we assume that the conditions (40)-(41) of Theorem III.3 hold. Then there exists $c(\theta) > 0$ so that the derivative of $V(\hat{x}) = \hat{x}^\top P \hat{x}$ (where P is a solution of (40)-(41)) along the trajectories of (69) satisfies

$$\dot{V}(t) \leq -\frac{c}{2} V(\hat{x}(t)) + 2\hat{x}(t)^\top PLC[\hat{x}(t - \tau) - \hat{x}(t)]. \quad (71)$$

Consequently, using $\hat{x}(t) - \hat{x}(t - \tau) = \int_{t-\tau}^t \dot{\hat{x}}(\ell) d\ell$, we obtain

$$\dot{V}(t) \leq -\frac{c}{2} V(\hat{x}(t)) - 2\hat{x}(t)^\top P(LCT(\theta))^2 \int_{t-2\tau}^{t-\tau} \hat{x}(\ell) d\ell - 2\hat{x}(t)^\top PLC T(\theta) \int_{t-\tau}^t [\theta \mathcal{A}^n(\Psi_n^\theta(\ell))] \hat{x}(\ell) d\ell. \quad (72)$$

Let Q be a symmetric positive definite matrix such that $Q^2 = P$. Then

$$\begin{aligned} \dot{V}(t) &\leq -\frac{c}{2} V(\hat{x}(t)) \\ &\quad + 2\bar{q}(\theta) \sqrt{V(\hat{x}(t))} \int_{t-2\tau}^{t-\tau} \sqrt{V(\hat{x}(\ell))} d\ell \\ &\quad + 2\sqrt{V(\hat{x}(t))} \int_{t-\tau}^t |q(\ell)| \sqrt{V(\hat{x}(\ell))} d\ell, \end{aligned} \quad (73)$$

where

$$q(\ell) = QLCT(\theta) [\theta \mathcal{A}^n(\Psi_n^\theta(\ell))] Q^{-1},$$

and

$$\bar{q}(\theta) = |Q(LCT(\theta))^2 Q^{-1}|.$$

Let

$$q^*(\theta) = \sup_s \{|q(s)|\}. \quad (74)$$

Since f is globally Lipschitz, then the constant q^* is well-defined. Then

$$\begin{aligned} \dot{V}(t) &\leq -\frac{c}{2} V(\hat{x}(t)) \\ &\quad + 2\bar{q} \int_{t-2\tau}^{t-\tau} \sqrt{V(\hat{x}(t))} \sqrt{V(\hat{x}(\ell))} d\ell \\ &\quad + 2q^* \int_{t-\tau}^t \sqrt{V(\hat{x}(t))} \sqrt{V(\hat{x}(\ell))} d\ell, \end{aligned} \quad (75)$$

Now, from Razumikhin's theorem, it follows that if

$$\tau < \varphi(\theta) \triangleq \frac{c(\theta)}{4(\bar{q}(\theta) + q^*(\theta))}, \quad (76)$$

then the origin of the system (69) is globally exponentially stable.

From Theorem III.3, the constant c is given by

$$c(\theta) = \frac{2\theta\lambda - 4k_{j_0} \lambda_{\max}(P)}{\lambda_{\max}(P)}, \quad (77)$$

where

$$\theta = \max\left(\sigma, \theta_{j_0}^{\frac{1}{1+j_0}}\right).$$

It is obvious that

$$\lim_{\theta \rightarrow +\infty} \frac{1}{\theta} c(\theta) = \frac{2\lambda}{\lambda_{\max}(P)}.$$

We can show by developing the expressions of $\bar{q}(\theta)$ and $q^*(\theta)$ that the following holds:

$$\lim_{\theta \rightarrow +\infty} \frac{1}{\theta} \bar{q}(\theta) = \lim_{\theta \rightarrow +\infty} \frac{1}{\theta} q^*(\theta) = +\infty.$$

Consequently,

$$\lim_{\theta \rightarrow +\infty} \varphi(\theta) = 0.$$

This means that the largest is θ , the smaller is the value of the tolerated delay τ . Thus the importance of the HG/LMI method provided in the previous section. Indeed, this latter provides smaller value of θ compared to the standard high-gain observer. This shows that the HG/LMI method is more performant than the standard high-gain method from the robustness point of view with respect to the delay in the output measurement.

B. Performance with respect to measurement noise

Since the problem of high-gain observer is the amplification of high-frequency measurement noise, we consider only the case where the measurement is affected by noises. That is why we consider the system

$$\begin{aligned} \dot{x}(t) &= Ax(t) + Bf(x(t)) \\ y(t) &= Cx(t) + \nu(t) \end{aligned} \quad (78)$$

with the corresponding state observer (11), where $\nu(t)$ represents the disturbance affecting the measurement $y(t)$. Therefore, the error dynamics (31) becomes:

$$\dot{\tilde{x}} = \theta \left(A(\Psi^\theta) - KC \right) \tilde{x} + \frac{1}{\theta^n} B \Delta f_1 - K \nu(t). \quad (79)$$

1) *An upper bound of the estimation error:* Here we give an upper bound on the estimation error in the case of the presence of noise in the measurements.

Theorem V.1. *Assume that there exist a positive definite and symmetric matrix P and a matrix Y of appropriate dimensions such that the inequalities (40)-(41) hold. Then with the observer gain L given by (44), there exist two positive constants α, β such that the estimation error $\tilde{x}(t)$ is upper bounded as follows:*

$$\|\tilde{x}(t)\| \leq \theta^{n-1} \max \left(\sqrt{\frac{\lambda_{\max}(P)}{\lambda_{\min}(P)}} \|e_0\| e^{-\gamma_1 \theta t}, \gamma_2 \|\nu(t)\| \right), \quad (80)$$

where

$$\gamma_1 = \frac{\beta}{2\lambda_{\max}(P)}, \quad \gamma_2 = \alpha \sqrt{\frac{\lambda_{\max}(P)}{\lambda_{\min}(P)}} \quad (81)$$

with

$$\alpha \geq \frac{2\lambda_{\max}(P) \|K\|}{\lambda - \frac{2\lambda_{\max}(P)}{\theta} k_{j_0}}, \quad (82)$$

$$\beta \leq \lambda - \frac{2\lambda_{\max}(P)}{\theta} \left(k_{j_0} + \frac{1}{\alpha} \|K\| \right). \quad (83)$$

Proof. The proof is standard and well known in the high-gain observer literature. We refer the reader to [28] and the references therein. Indeed, after developing the calculation of \dot{V} along the trajectory of (78), the key of the proof is based on the fact that under the conditions (40)-(41), if $\|\hat{x}(t)\| \geq \alpha\|\nu(t)\|$ for $\alpha > 0$ satisfying (82), then there exists $\beta > 0$ satisfying (83) such that $\dot{V}(\hat{x}(t)) \leq -\beta\theta\|\hat{x}(t)\|^2$. Therefore, using the fact that

$$\lambda_{\min}(P)\|\hat{x}(t)\|^2 \leq V(\hat{x}(t)) \leq \lambda_{\max}(P)\|\hat{x}(t)\|^2,$$

we can easily deduce that when

$$V(\hat{x}(t)) \geq \lambda_{\max}(P)\alpha^2\|\nu(t)\|^2,$$

we obtain

$$\|\hat{x}(t)\| \leq \sqrt{\frac{\lambda_{\max}(P)}{\lambda_{\min}(P)}}\|\hat{x}_0\|e^{-\gamma_1\theta t}, \quad (84)$$

where γ_1 is given in (81). On the other hand, by inverse implication, we can deduce that if there exists $t \geq 0$ such that $\|\hat{x}(t)\| > \sqrt{\frac{\lambda_{\max}(P)}{\lambda_{\min}(P)}}\|\hat{x}_0\|e^{-\gamma_1\theta t}$, then we have $V(\hat{x}(t)) < \lambda_{\max}(P)\alpha^2\|\nu(t)\|^2$, which leads to

$$\|\hat{x}(t)\| < \alpha\sqrt{\frac{\lambda_{\max}(P)}{\lambda_{\min}(P)}}\|\nu(t)\|.$$

Consequently,

$$\|\tilde{x}(t)\| \leq \theta^{n-1} \max\left(\sqrt{\frac{\lambda_{\max}(P)}{\lambda_{\min}(P)}}\|e_0\|e^{-\gamma_1\theta t}, \gamma_2\|\nu(t)\|\right),$$

which ends the proof. \square

2) *Comments and comparisons:* Notice that compared to the standard high-gain observer, the upper bound of $\|\tilde{x}(t)\|$ is smaller because of the smaller value of the lower bound of the tuning parameter θ corresponding to the HG/LMI method. To get a precise idea, assume that the tuning parameter θ takes the smallest value, namely θ_0 for the standard high-gain observer, and $\max\left(\sigma, \theta_{j_0}^{\frac{1}{1+j_0}}\right)$ for the HG/LMI observer. Then, we get

$$\limsup_{t \rightarrow +\infty} \|\tilde{x}(t)\| \leq \gamma_{\text{HG}}\theta_0^{n-1} \limsup_{t \rightarrow +\infty} \|\nu(t)\| \quad (85)$$

with the standard high-gain observer, and

$$\limsup_{t \rightarrow +\infty} \|\tilde{x}(t)\| \leq \gamma_2 \max\left(\sigma, \theta_{j_0}^{\frac{1}{1+j_0}}\right)^{n-1} \limsup_{t \rightarrow +\infty} \|\nu(t)\| \quad (86)$$

with the HG/LMI observer, where γ_{HG} in (85) is the constant given by the same formula as in (81) with the corresponding Lyapunov matrix P in the standard high-gain case.

Since in general the parameter σ is smaller than the threshold value related to the high-gain constraint, then we have

$$\max\left(\sigma, \theta_{j_0}^{\frac{1}{1+j_0}}\right) = \theta_{j_0}^{\frac{1}{1+j_0}}.$$

Therefore, inequality (86) is rewritten as

$$\limsup_{t \rightarrow +\infty} \|\tilde{x}(t)\| \leq \gamma_2 \theta_{j_0}^{\frac{n-1}{1+j_0}} \limsup_{t \rightarrow +\infty} \|\nu(t)\|. \quad (87)$$

It is quite clear that the upper bound of the error corresponding to the HG/LMI observer is smaller than that of the standard high-gain observer since $\theta_{j_0}^{\frac{1}{1+j_0}}$ is smaller than θ_0 because of the power $\frac{1}{1+j_0}$ and the fact that the difference between γ_2 and γ_{HG} is not significative compared to the difference between the powers. In the case of standard high-gain observer, this power corresponds to $j_0 = 0$, which is the biggest one.

Analytically, the comparison is more clear if Assumption III.1 holds. Indeed, in such a case, we have

$$\sigma = 1 \text{ and } \theta_{j_0} = \theta_0,$$

which means that

$$\max\left(\sigma, \theta_{j_0}^{\frac{1}{1+j_0}}\right) = \theta_0^{\frac{1}{1+j_0}}.$$

Clearly, with the same threshold θ_0 , the power corresponding to the HG/LMI observer is $\frac{n-1}{1+j_0}$ instead of $n-1$ for the standard high-gain observer.

Recently, a new high-gain observer with limited gain power was proposed in [28] and [31]. The corresponding observer structure is different from that used in this paper. Indeed, the authors in [28] proposed a novel observer structure, which is a kind of interconnected system of dimension $2n-2$. Although their gain power is limited to 2 instead of n for the standard high-gain observer and the HG/LMI technique, it is worth noticing that there are two drawbacks related to this interconnected structure:

- The higher dimension of the observer ($2n-2$ instead of n) may increase significantly the threshold θ_0 of the tuning parameter, as shown through the numerical example in Table V. This is due to the higher dimension of the Lyapunov matrix and the algorithm providing the gain K by using a block-tridiagonal higher dimensional matrix.
- Even if the gain power is limited to 2, the upper bound and the power $n-1$ in the estimation error remains the same as that of the standard high-gain observer. Indeed, with the *Astolfi/Marconi* observer in [28], we get

$$\limsup_{t \rightarrow +\infty} \|\tilde{x}(t)\| \leq \gamma_{\text{AM}}\ell^{kn-1} \limsup_{t \rightarrow +\infty} \|\nu(t)\|, \quad (88)$$

where γ_{AM} is a constant similar to γ_2 in (81) with appropriate Lyapunov matrix of dimension $2n-2$. The explicit value of this constant can be found in [28].

In fact, although the observer uses only θ and θ^2 , but owing of the interconnected form the parameter θ is diffused and redistributed in all the components of the system and then the term θ^{n-1} reappears in the bounds (80) and (85). The interconnected form of the observer only makes it possible to hide the higher powers of θ .

On the other hand, the *Astolfi/Marconi* observer may be interesting if some saturations are added to the observer [37]. It can avoid the peaking phenomenon thanks to the interconnected structure of the observer, which allows a possibility of saturations in various steps. Nevertheless, it is important to notice that the HG/LMI technique, notably the decomposition of the nonlinear function as in (30), can formally be applied to the *Astolfi/Marconi* observer to enhance performances. The only obstacle we have to face is the computation of

the Lyapunov matrix P and the gain K from the block-tridiagonal matrix, which becomes non tridiagonal because of the injected nonlinear terms due to the application of the HG/LMI methodology. This is one of the future work we aim to investigate by using rigorous arguments. At this stage, we focus our study on the HG/LMI technique and its advantages compared to the standard high-gain observer.

Remark 6. *The advantage of the proposed observer lies in its ability to combine the standard High-gain observer and LMI-based observer. Then, it can use the advantages of each of the two methodologies. Since the LMI-based observer do not have the "peaking phenomenon", then also the new observer can do the same. Indeed, to avoid the peaking phenomenon, it suffices to increase the value of the compromise index j_0 in order to decrease the value of θ . As stated in the paper, both LPV/LMI-based technique and standard high-gain observer can be viewed as particular cases of the proposed HG/LMI observer. The latter is able to avoid the peaking phenomenon, to reduce the sensitivity to high-frequency measurement noise, and to enhance the convergence rate if necessary. To get a good tradeoff between all these criteria, the new observer offers the possibility to play with the values of j_0 and θ .*

VI. AN ILLUSTRATIVE EXAMPLE

We show through a numerical example the clear advantages of combining the high gain and LMI observer design methods by illustrating how the size of the observer gain varies for different values of j_0 .

We consider the case of a five dimensional system with a nonlinearity

$$f(x) = \frac{k_f}{5} \sum_{i=1}^5 \sin(x_i).$$

This nonlinearity satisfies (7) and (22) with $\gamma_f = k_f$. We can show easily that

$$k_{j_0} = \frac{k_f(5 - j_0)}{5}.$$

We will provide some comparisons between the standard high-gain, the Astolfi/Marconi observer, and the proposed HG/LMI technique. The advantage of the "compromise index" j_0 will be shown for different values of k_f . Table V illustrates how the values of the proposed HG/LMI observer gain are smaller than those of the standard high-gain observer and Astolfi/Marconi observer.

Notice that the LPV/LMI technique, which corresponds to $j_0 = 5$, provides lower observer gains, but we need to solve $2^5 = 32$ LMIs. However, this high number of LMIs would complicate the numerical solving of these LMIs for higher dimensional systems. This can lead to infeasible LMIs. Hence the importance of the Proposed HG/LMI method. For instance, it suffices to solve 2 LMIs instead of only one to reduce significantly the value of θ from $\theta = 31.72$ to $\theta = 5.25$ for $k_f = 1$ and from $\theta = 273.03$ to $\theta = 17.63$ for $k_f = 10$. We can reduce more the observer gain, but we have to solve more LMIs, as can be shown in Table V (4 LMIs for $j_0 = 2$ and 8 LMIs for $j_0 = 3$). This is the reason why the index j_0 is called the "compromise index".

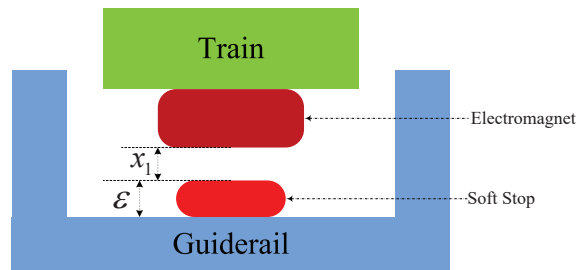


Fig. 1. Schematic of levitation system at each electromagnet

To have an idea of the difference between the standard high-gain and the HG/LMI observer, we take for instance $k_f = 0.1$. Then we obtain the following gains for different values of j_0 :

$$L_0 = \begin{bmatrix} 17.40 \\ 148.20 \\ 753.30 \\ 2216.10 \\ \boxed{3047.10} \end{bmatrix} \quad L_1 = \begin{bmatrix} 7.21 \\ 25.73 \\ 54.99 \\ 68.74 \\ \boxed{40.93} \end{bmatrix}$$

$$L_2 = \begin{bmatrix} 5.16 \\ 13.24 \\ 20.48 \\ 18.77 \\ \boxed{8.45} \end{bmatrix} \quad L_3 = \begin{bmatrix} 4.17 \\ 8.67 \\ 10.98 \\ 8.41 \\ \boxed{3.39} \end{bmatrix}$$

for $\sigma = 1.5$, $\sigma = 1.5$, and $\sigma = 1.2$, respectively for $j_0 = 1, 2, 3$. L_0 is the standard high-gain, which corresponds to $j_0 = 0$.

We can see that for $j_0 = 1, 2, 3$, the last component of the gain L_{j_0} is not necessarily higher than the other components, contrarily to the standard high-gain L_0 for which this increasing property is necessarily fulfilled. This is due to the fact that in the HG/LMI methodology, the LMIs (40) depend on σ , which can affect the gain K and provides smaller values in the last components.

VII. APPLICATION TO MAGNETIC LEVITATION SYSTEMS FOR TRAINS

Now we study a real-world example as an application of the proposed observer design methodology. We consider the model of a magnetic levitation system for trains, see Fig. 1, in which the objective is to control the electromagnet's position at a desired height above the guidrail. The dynamics of this magnetic levitation system are typically described using the position x_1 , velocity and current in the electromagnet as the states. In this paper, we use instead the transformed states of position, velocity and acceleration which lead to plant dynamics of the following form:

$$\begin{cases} \dot{x}_1 = x_2 \\ \dot{x}_2 = x_3 \\ \dot{x}_3 = -\frac{2[R(x_1+\epsilon)+L_1x_2](x_3+g)}{L_1(x_1+\epsilon)+L_0z_0} \\ \quad + \frac{2\sqrt{\frac{K}{m}}(x_3+g)}{L_1(x_1+\epsilon)+L_0z_0}u \triangleq f(x, u) \\ y = x_1 \end{cases}, \quad (89)$$

Standard High-Gain observer									
j_0	k_f	θ_0	K						
0	1	31.72	5.66	13.12	16.49	11.12	3.42		
	10	273.03	12.07	33.47	45.54	31.58	9.92		
	100	2594.20	32.51	97.87	137.15	96.01	30.39		

Astolfi/Marconi observer of dimension 8										
j_0	k_f	ℓ^*	K_1		K_2		K_3		K_4	
0	1	273.29	2.9	8.0629	2.9	3.0221	2.9	1.3425	2.9	0.5032
	10	2732.90	2.9	8.0629	2.9	3.0221	2.9	1.3425	2.9	0.5032
	100	27329.09	2.9	8.0629	2.9	3.0221	2.9	1.3425	2.9	0.5032

HG/LMI observer									
j_0	k_f	n_{LMI}	σ	$\theta \frac{1+j_0}{j_0}$	K				
1	1	2	5.2	5.25	5.38	12.32	15.54	10.71	3.51
	10		17.5	17.63	5.46	12.77	16.61	12.10	4.51
	100		62	62	11.43	34.53	53.42	46.94	24.56
2	1	4	2.5	2.88	5.11	11.57	14.74	10.65	4.08
	10		7	7.06	5.34	12.86	17.89	15.08	7.92
	100		23	24.32	6.22	18.01	32.19	40.23	39.86
3	1	8	2	2.06	4.73	10.34	13.03	9.67	4.19
	10		4.10	4.47	5.22	12.83	19.04	18.62	13.31
	100		14	15.12	6.92	23.02	50.57	86.80	133.18

TABLE V
COMPARISONS BETWEEN THE HIGH-GAIN OBSERVERS FOR DIFFERENT VALUES OF k_f .

where x_1 , x_2 and x_3 are the position, velocity and acceleration respectively of the electromagnet, $x = [x_1, x_2, x_3]^T$, u is the control input voltage, and y is the measurement output which may be perturbed by measurement noise and/or disturbance. While the position of the electromagnet above the rail is measured, the velocity and current could be estimated using an observer. All the system parameters used for simulations together with the original system model can be found in [38]. The state transformation procedure as well as the Lipschitz constant computation of $f(x, u)$ are given in the Appendix of this paper. In order to carry out simulations below, the parameter values are $g = 9.81$, $m = 11.87 \times 10^{-3}$, $R = 28.7$, $L_1 = 65$, $L_{oz_0} = 0.065$, $K = 1.4 \times 10^{-2}$, $\epsilon = 0.01$. Here we let the initial state be $x(0) = [0.1, 0, 0]^T$ and use a constant voltage input $u = 9$ to activate the system. Then, we can compute the Lipschitz constant of $f(x, u)$ to be 195.8713. Before moving on, we impose a constraint on the system (89) by letting $f(x, u) \equiv 0$ when $x_3 + g < 0$. This makes sense in practice because $x_3 + g$ can never become negative due to the physical stop and due to the current never becoming negative in the provided electrical hardware.

a) First, we design a standard high-gain observer for the system (89) following Theorem II.2. Without any loss of generality, we let $\lambda = 1$ throughout this paper. By using Matlab & YALMIP, we can easily obtain that $Y = [0.5997, 1.4077, -0.4068]^T$, $\theta = 796.8498$ and

$$P = \begin{bmatrix} 1.6018 & -0.5976 & -0.4264 \\ -0.5976 & 0.6184 & -0.5944 \\ -0.4264 & -0.5944 & 1.6133 \end{bmatrix}$$

are solutions to (24) and (25). Then we get $K =$

$P^{-1}Y^T = [45.6461, 89.4081, 44.7584]^T$ and $L = 10^{10} \cdot [0, 0.0057, 2.2647]^T$ through (19). Obviously, this observer with an extremely high gain is not suitable for implementation and thus the corresponding simulation is omitted.

b) Next, we turn to the high-gain observer proposed in [28]. We assign the eigenvalues of the M matrix (see (7) therein) to be -1 , -1.3 , -1.6 and -1.9 , and then derive that $K_1 = [2.9, 3.98]^T$ and $K_2 = [2.9, 0.993]^T$. Hence M is known as well. By solving $PM + M^T P = -I$, we obtain

$$P = \begin{bmatrix} 2.0685 & -1.3815 & 0.3815 & -1.8960 \\ -1.3815 & 1.3314 & -0.0830 & 1.1302 \\ 0.3815 & -0.0830 & 0.7306 & -1.6302 \\ -1.8960 & 1.1302 & -1.6302 & 5.4133 \end{bmatrix},$$

and thus $\ell^* = 2798.8$.

c) Finally, the observer proposed in this paper will be designed for the system (89). Here we skip the details of the involved computation due to limited space. To reduce the high-gain, we choose as compromise index $j_0 = 2$, then we obtain $\theta = 99$ and $K = [68, 386.8, 1097.8]^T$. This is another advantage of the "compromise index" j_0 .

Denote $\hat{x}_{\text{AM}} = [\hat{x}_{1,\text{AM}}, \hat{x}_{2,\text{AM}}, \hat{x}_{3,\text{AM}}]^T$ and $\hat{x}_{\text{LL}} = [\hat{x}_{1,\text{LL}}, \hat{x}_{2,\text{LL}}, \hat{x}_{3,\text{LL}}]^T$ as the state estimates for the system (89) by using the observer design methods proposed in [28]¹ and in the present paper, respectively. Let $\hat{x}_{\text{AM}}(0) = [0.5, 0, 0]^T$ and $\hat{x}_{\text{LL}}(0) = [0.5, 0, 0]^T$. In Fig. 2, the six curves of the absolute values $|\hat{x}_{i,\text{AM}} - x_i|$ and $|\hat{x}_{i,\text{LL}} - x_i|$, $i = 1, 2, 3$, are plotted. The two observers work for the system (89) and it is

¹The dimension of this observer is in fact 4. \hat{x}_{AM} is obtained by "extracting" 3 components from its states, whose initial values are $[0.5, 0, 0, 0]^T$. The reader can refer to [28] for more details.

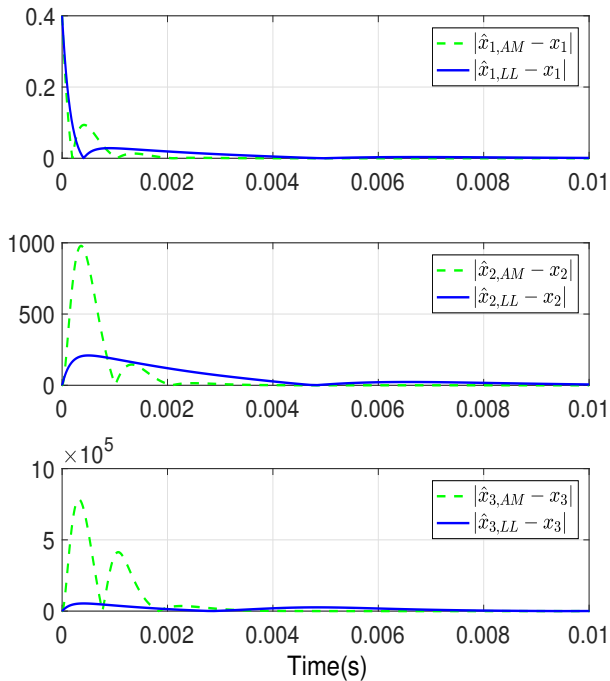


Fig. 2. Absolute values of estimation errors

clear that both trajectories of estimation errors approach zeros. Note, however, that the transient performance of our designed observer is much better in particular for the estimation of x_2 and x_3 , although the convergence speeds are almost the same.

In addition, the simulation is also done using an additive measurement noise, which is a Gaussian distributed random signal with mean zero and standard deviation 0.01. The simulation results are given in Fig. 3. From the plots of the norms of the estimation errors, we know that on the whole our designed observer still works much better than the one in [28].

Besides measurement noise, we consider a single pulse disturbance signal, which lasts for 0.002s with magnitude 0.3 and is injected into the measurement output at 0.03s. It follows from Fig. 4 that our designed observer moves back to the steady state faster. We also note that the estimation of x_2 and x_3 is not perturbed that much.

Finally, we want to stress that the above advantages hold under our designed observer with a dimension of just 3 rather than the observer with dimension 4 proposed in [28] for the system (89).

VIII. CONCLUSIONS

In this paper we presented a new state observer design for a class of triangular systems with Lipschitz nonlinearities. This new observer, called HG/LMI observer, has the advantage to provide lower gain compared to the standard high-gain observer. The key idea behind this observer is based on the use of the LPV/LMI technique to modify the high-gain constraint, which reduces significantly the Lipschitz constant and leads

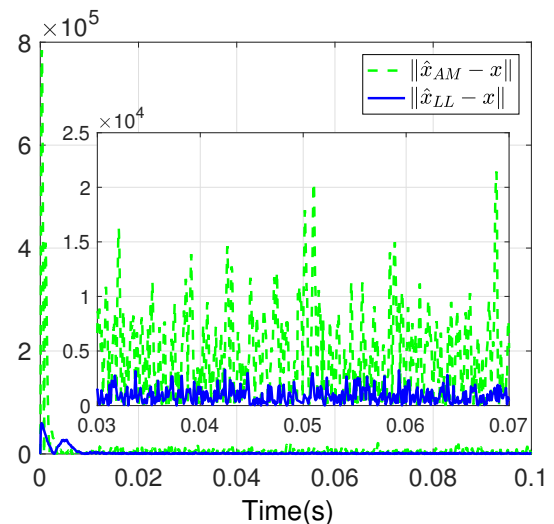


Fig. 3. Norms of estimation errors with measurement noise

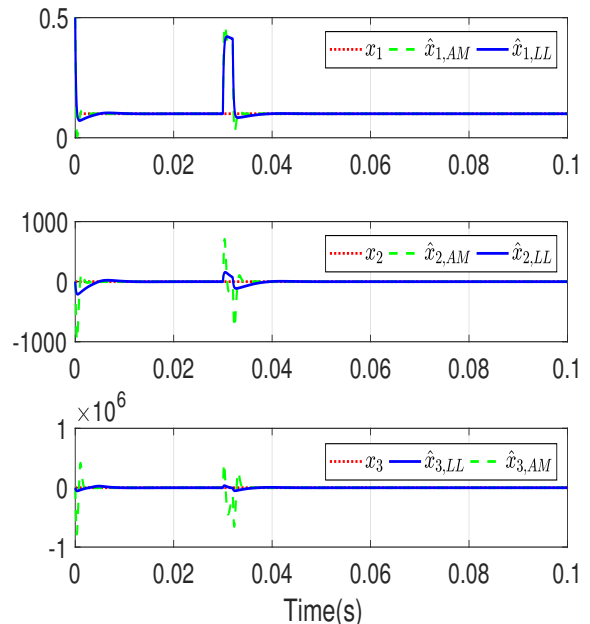


Fig. 4. Estimation states with a single pulse

to smaller observer gains compared to the classical high-gain. A systematic design algorithm was provided and extensions to multi nonlinear functions was developed, together with analysis of performance in the presence of noise and in the presence of time delayed measurement. A numerical example was used to show the effectiveness of the HG/LMI technique, especially the variation in gain size with change in the compromise index. To show the applicability of the proposed observer, an application to magnetic levitation system for trains was provided.

Solving observer-based output feedback stabilization problem by using the proposed state observer is one of the future work we aim to investigate in a deepen way. All the robustness

and performance issues related to output feedback control using the HG/LMI observer will be carefully investigated.

APPENDIX

The magnetic levitation system in [38] is given by

$$m\ddot{x}_1 = K \frac{I^2}{(x_1 + \epsilon)^2} - mg, \quad (\text{A.1})$$

$$u = RI + \frac{d}{dt}(L(x_1)I), \quad (\text{A.2})$$

$$L(x_1) = L_1 + \frac{L_0 z_0}{x_1 + \epsilon}, \quad (\text{A.3})$$

where I is the current in the coil of the electromagnet, other variables and parameters have been introduced in Section VII. Substituting (A.3) into (A.2) yields

$$RI + L(x_1) \frac{dI}{dt} - \frac{L_0 z_0 I}{(x_1 + \epsilon)^2} \dot{x}_1 = u.$$

Conventionally, the state space vector is chosen as $[x_1, \dot{x}_1, I]^\top$. It results in the following state space dynamics

$$\frac{d}{dt} \begin{bmatrix} x_1 \\ \dot{x}_1 \\ I \end{bmatrix} = \begin{bmatrix} 0 & 1 & 0 \\ 0 & 0 & 0 \\ 0 & 0 & 0 \end{bmatrix} \begin{bmatrix} x_1 \\ \dot{x}_1 \\ I \end{bmatrix} + \begin{bmatrix} 0 \\ -1 \\ 0 \end{bmatrix} g + \begin{bmatrix} 0 \\ \frac{KI^2}{m(x_1 + \epsilon)^2} \\ -\frac{R}{L(x_1)} I + \frac{L_0 z_0 I}{(x_1 + \epsilon)^2 L(x_1)} \dot{x}_1 \end{bmatrix} + \begin{bmatrix} 0 \\ 0 \\ \frac{1}{L(x_1)} \end{bmatrix} u. \quad (\text{A.4})$$

In order to convert (A.4) to the observable canonical form, we choose the new state space vector as

$$x = \begin{bmatrix} x_1 & \dot{x}_1 & \frac{K}{m} \frac{I^2}{(x_1 + \epsilon)^2} - g \end{bmatrix}^\top.$$

Then, the observable canonical form is given by

$$\dot{x} = \begin{bmatrix} 0 & 1 & 0 \\ 0 & 0 & 1 \\ 0 & 0 & 0 \end{bmatrix} x + \begin{bmatrix} 0 \\ 0 \\ \frac{2K}{m} \left\{ \left(-1 + \frac{L_0 z_0}{(x_1 + \epsilon)L(x_1)} \right) \frac{I^2 \dot{x}_1}{(x_1 + \epsilon)^3} - \frac{RI^2}{L(x_1)(x_1 + \epsilon)} \right\} \end{bmatrix} + \begin{bmatrix} 0 \\ 0 \\ \frac{2KI}{L(x_1)m(x_1 + \epsilon)} \end{bmatrix} u.$$

From $x_3 = \frac{K}{m} \frac{I^2}{(x_1 + \epsilon)^2} - g$, we get $I = (x_1 + \epsilon) \sqrt{\frac{m}{K}(x_3 + g)}$. Therefore, we obtain the model (89).

The Lipschitz constant of $f(x, u)$ can be computed by calculating its partial derivatives

$$\frac{\partial f(x, u)}{\partial x_1} = \frac{2(L_1^2 x_2 - RL_0 z_0)(x_3 + g)}{[L_1(x_1 + \epsilon) + L_0 z_0]^2} - \frac{2L_1 \sqrt{\frac{K}{m}(x_3 + g)}}{[L_1(x_1 + \epsilon) + L_0 z_0]^2} u,$$

$$\frac{\partial f(x, u)}{\partial x_2} = -\frac{2L_1(x_3 + g)}{L_1(x_1 + \epsilon) + L_0 z_0},$$

$$\frac{\partial f(x, u)}{\partial x_3} = -\frac{2[R(x_1 + \epsilon) + L_1 x_2]}{L_1(x_1 + \epsilon) + L_0 z_0} + \frac{\sqrt{\frac{K}{m(x_3 + g)}}}{L_1(x_1 + \epsilon) + L_0 z_0} u,$$

and finding out the supremum on

$$\left\| \left[\frac{\partial f(x, u)}{\partial x_1}, \frac{\partial f(x, u)}{\partial x_2}, \frac{\partial f(x, u)}{\partial x_3} \right] \right\|$$

over a sufficiently long time interval under a given control input through numerical simulation. As in Section VII, we use a constant voltage input $u = 9$. Then it is easy to perform the computations and find the Lipschitz constant as 195.8713.

ACKNOWLEDGEMENTS

The authors would like to thank the anonymous reviewers and Associate Editor for their constructive comments and suggestions, which have significantly improved the quality of the paper. The first author thanks EPI-Inria DISCO for supporting the preliminary result of this paper. The second author thanks the financial support from the State Key Laboratory of Intelligent Control and Decision of Complex Systems, the National Natural Science Foundation of China (Grant No. 61703099), and the China Postdoctoral Science Foundation (Grant No. 2017M621589). The fourth author (R. Rajamani) acknowledges funding from NSF Grant CMMI 1562006 for a portion of this work.

REFERENCES

- [1] A. J. Krener and W. Respondek, "Nonlinear observer with linearizable error dynamics," *SIAM J. Control and Optimization*, vol. 23, no. 2, pp. 197–216, 1985.
- [2] D. Simon, "A game theory approach to constrained minmax state estimation," *IEEE Trans. on Signal Processing*, vol. 54, no. 2, pp. 405–412, 2006.
- [3] J. Gauthier, H. Hammouri, and S. Othman, "A simple observer for nonlinear systems applications to bioreactors," *IEEE Trans. on Automatic Control*, vol. 37, no. 6, pp. 875–880, 1992.
- [4] R. Rajamani, "Observers for Lipschitz nonlinear systems," vol. 43, no. 3, pp. 397–401, 1998.
- [5] H. Khalil, *Nonlinear Systems*. Prentice Hall, Upper Saddle River, NJ, 2002.
- [6] M. Arcak and P. Kokotovic, "Observer-based control of systems with slope-restricted nonlinearities," *IEEE Transactions on Automatic Control*, vol. 46, no. 7, pp. 1146–1150, 2001.
- [7] C. Kravaris, V. Sotiropoulos, C. Georgiou, N. Kazantzis, M. Q. Xiao, and A. J. Krener, "Nonlinear observer design for state and disturbance estimation," in *2004 American Control Conference ACC'04*, Boston, Massachusetts, USA, June 2004.
- [8] R. Rajamani, *Vehicle Dynamics and Control*. 2nd edition, Springer Verlag, 2012.
- [9] R. Rajamani, H. Tan, B. Law, and W. Zhang, "Demonstration of integrated longitudinal and lateral control for the operation of automated vehicles in platoons," vol. 8, no. 4, pp. 695–708, 2000.
- [10] H. Hammouri, M. Kinnaert, and E. H. E. Yaagoubi, "Observer-based approach to fault detection and isolation for nonlinear systems," *IEEE Transactions on Automatic Control*, vol. 44, no. 10, pp. 1879–1884, Oct 1999.
- [11] S. Ibrir, "Circle-criterion approach to discrete-time nonlinear observer design," *Automatica*, vol. 43, no. 8, pp. 1432–1441, 2007.
- [12] A. Zemouche, M. Boutayeb, and G. I. Bara, "Observers for a class of Lipschitz systems with extension to \mathcal{H}_∞ performance analysis," *Systems & Control Letters*, vol. 57, no. 1, pp. 18–27, 2008.

- [13] M. Abbaszadeh and H. J. Marquez, "Nonlinear observer design for one-sided Lipschitz systems," in *IEEE American Control Conference*, Baltimore, MD, USA, July 2010.
- [14] G. Phnomchoeng and R. Rajamani, "Nonlinear observer for bounded jacobian systems, with applications to automotive slip angle estimation," *IEEE Transactions on Automatic Control*, vol. 56, no. 5, pp. 1163–1170, 2011.
- [15] M. Chong, R. Postoyan, D. Nesić, L. Kuhlmann, and A. Varsavsky, "A robust circle criterion observer with application to neural mass models," *Automatica*, vol. 48, no. 11, pp. 2986–2989, 2012.
- [16] B. Açikmese and M. Corless, "Observers for systems with nonlinearities satisfying incremental quadratic constraints," *Automatica*, vol. 47, no. 7, pp. 1339–1348, 2011.
- [17] M. Oueder, M. Farza, R. B. Abdenmour, and M. M'Saad, "A high gain observer with updated gain for a class of MIMO non-triangular systems," *Systems & Control Letters*, vol. 61, no. 2, pp. 298–308, 2012.
- [18] A. Zemouche and M. Boutayeb, "On LMI conditions to design observers for Lipschitz nonlinear systems," *Automatica*, vol. 49, no. 2, pp. 585–591, 2013.
- [19] Y. Wang, R. Rajamani, and D. Bevy, "Observer design for parameter varying differentiable nonlinear systems, with application to slip angle estimation," *IEEE Transactions on Automatic Control*, vol. 62, no. 4, pp. 1940–1945, 2017.
- [20] J. Gauthier and I. Kupka, "Observability and observers for nonlinear systems," *SIAM J. on Control and Optimization*, vol. 32, no. 4, pp. 975–994, 1994.
- [21] H. Khalil and L. Praly, "High-gain observers in nonlinear feedback control," *Int. Journal of Robust and Nonlinear Control*, vol. 24, no. 6, pp. 993–1015, 2014.
- [22] J. Ahrens and H. Khalil, "High-gain observers in the presence of measurement noise: a switched-gain approach," *Automatica*, vol. 45, no. 4, pp. 936–943, 2009.
- [23] N. Boizot, E. Busvelle, and J. Gauthier, "An adaptive high-gain observer for nonlinear systems," *Automatica*, vol. 46, no. 9, pp. 1483–1488, 2010.
- [24] V. Andrieu, L. Praly, and A. Astolfi, "High gain observers with updated gain and homogeneous correction terms," *Automatica*, vol. 45, no. 2, pp. 422–428, 2009.
- [25] C. Prieur, S. Tarbouriech, and L. Zaccarian, "Hybrid high-gain observers without peaking for planar nonlinear systems," in *51st IEEE Conference on Decision and Control*, Maui, Hawaii, USA, 2012, pp. 6175–6180.
- [26] A. Alessandri and A. Rossi, "Time-varying increasing-gain observers for nonlinear systems," *Automatica*, vol. 49, no. 9, pp. 2845–2852, 2013.
- [27] —, "Increasing-gain observers for nonlinear systems: stability and design," *Automatica*, vol. 57, no. 7, pp. 180–188, 2015.
- [28] D. Astolfi and L. Marconi, "A high-gain nonlinear observer with limited gain power," *IEEE Transactions on Automatic Control*, vol. 60, no. 11, pp. 3059–3064, 2015.
- [29] A. Zemouche, "Observer design for nonlinear systems by using high-gain and LPV/LMI-based technique," in *IEEE American Control Conference*, Seattle, WA, USA., May 2017.
- [30] S. Boyd, L. El Ghaoui, E. Feron, and V. Balakrishnan, *Linear Matrix Inequalities in System and Control Theory*, ser. Studies in Applied Mathematics. Philadelphia, PA: SIAM, 1994, vol. 15.
- [31] L. Wang, D. Astolfi, L. Marconi, and H. Su, "High-gain observers with limited gain power for systems with observability canonical form," *Automatica*, vol. 75, no. 1, pp. 16–23, 2017.
- [32] J. Gauthier and I. Kupka, *Deterministic Observation Theory and Applications*. Cambridge University Press, Cambridge, UK, 2004.
- [33] R. Sanfelice and L. Praly, "Convergence of nonlinear observers on \mathbb{R}^n with a Riemannian metric (Part I)," *IEEE Transactions on Automatic Control*, vol. 57, no. 7, pp. 1709–1722, 2012.
- [34] —, "Convergence of nonlinear observers on \mathbb{R}^n with a Riemannian metric (Part II)," *IEEE Transactions on Automatic Control*, vol. 61, no. 10, pp. 2848–2860, 2016.
- [35] —, "Nonlinear observer design with an appropriate Riemannian metric," in *48th IEEE Conference on Decision and Control and 28th Chinese Control Conference*, Shanghai, China, 2009, pp. 6514–6519.
- [36] A. Zemouche, R. Rajamani, B. Boukroune, H. Rafaralahy, and M. Zasadzinski, "Convex optimization based dual gain observer design for Lipschitz nonlinear systems," in *IEEE American Control Conference*, Boston, MA, USA., July 2016.
- [37] D. Astolfi, L. Marconi, and A. Teel, "Low-power peaking-free high-gain observers for nonlinear systems," in *European Control Conference*, Aalborg, Denmark., June 2016.
- [38] N. Al-Muthairi and M. Zribi, "Sliding mode control of a magnetic levitation system," *Mathematical Problems in Engineering*, vol. 2004, no. 2, pp. 93–107, 2004.



Ali ZEMOUCHE received his Ph.D. degree in automatic control in 2007, from the University Louis Pasteur, Strasbourg, France, where he held post-doctorate degree from october 2007 to august 2008. Dr. Zemouche joined, as an Associate Professor, the Centre de Recherche en Automatique de Nancy (CRAN UMR CNRS 7039) at the Université de Lorraine, since September 2008. He held an academic position at Inria-Saclay (EPI DISCO) from September 2016 to august 2017. His research activities include nonlinear systems, state observers, observer-based control, time-delay systems, robust control, and application to real-world models. Dr Zemouche is Associate Editor for several international journals: *SIAM Journal of Control and Optimization*; *European Journal of Control*; *IEEE Access*; *Cogent Engineering*; and *Designs (MDPI Journal)*. He is also a member of the Conference Editorial Board of *IEEE Control Systems Society* and *IFAC TC2.3 (Non-Linear Control Systems)*. He is organizer of several Invited Sessions in international conferences and served as managing guest editor for a Special Issue in *European Journal of Control*.

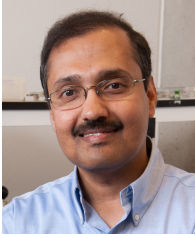


Fan ZHANG received the B.S. degree in Automation in 2008 and the M.S. degree in Flight Vehicle Design in 2010, both from Harbin Institute of Technology, China. He received the Ph.D. degree in Systems and Control from University of Groningen, the Netherlands in 2015. His research interests include the control and estimation of cyber-physical systems and multi-agent networks.



Frédéric MAZENC received his PhD in Automatic Control and Mathematics from the CAS at Ecole des Mines de Paris in 1996. He was a Postdoctoral Fellow at CESAME at the University of Louvain in 1997. From 1998 to 1999, he was a Postdoctoral Fellow at the Centre for Process Systems Engineering at Imperial College. He was a CR at INRIA Lorraine from October 1999 to January 2004. From 2004 to 2009, he was a CRI at INRIA Sophia-Antipolis. Since 2010, he has been a CRI at INRIA Saclay. He received a best paper award from the IEEE

Transactions on Control Systems Technology at the 2006 IEEE Conference on Decision and Control. His current research interests include nonlinear control theory, differential equations with delay, robust control, and microbial ecology. He has more than 200 peer reviewed publications. Together with Michael Malisoff, he authored a research monograph entitled *Constructions of Strict Lyapunov Functions in the Springer Communications and Control Engineering Series*.



Rajesh RAJAMANI obtained his M.S. and Ph.D. degrees from the University of California at Berkeley in 1991 and 1993 respectively and his B.Tech degree from the Indian Institute of Technology at Madras in 1989. Dr. Rajamani is currently Professor of Mechanical Engineering at the University of Minnesota. His active research interests include sensors and estimation systems for automotive and biomedical applications. Dr. Rajamani has co-authored over 130 journal papers and is a co-inventor on 13 patent applications. He is the author of the popular book

"Vehicle Dynamics and Control" published by Springer Verlag. Dr. Rajamani has served as Chair of the IEEE Technical Committee on Automotive Control and on the editorial boards of the IEEE Transactions on Control Systems Technology, the IEEE/ASME Transactions on Mechatronics, and the IEEE Control Systems Magazine. Dr. Rajamani is a Fellow of ASME and has been a recipient of the CAREER award from the National Science Foundation, the 2001 Outstanding Paper award from the journal IEEE Transactions on Control Systems Technology, the Ralph Teetor Award from SAE, and the 2007 O. Hugo Schuck Award from the American Automatic Control Council.